Dynamics of Fullerene Coalescence

Yong-Hyun Kim,[1,*] In-Ho Lee,[2] K. J. Chang,[1] and Sangsan Lee[3]

[1]*Department of Physics, Korea Advanced Institute of Science and Technology, Daejeon 305-701, Korea*
[2]*Korea Research Institute of Standards and Science, Daejeon 305-600, Korea*
[3]*Korea Institute of Science and Technology Information, Daejeon 305-333, Korea*

Fullerene coalescence experimentally found in fullerene-embedded single-wall nanotubes under electron-beam irradiation or heat treatment is simulated by minimizing the classical action for many atom systems. The dynamical trajectory for forming a (5,5) C_{120} nanocapsule from two C_{60} fullerene molecules consists of thermal motions around potential basins and ten successive Stone-Wales–type bond rotations after the initial cage-opening process for which energy cost is about 8 eV. Dynamical paths for forming large-diameter nanocapsules with (10,0), (6,6), and (12,0) chiral indexes have more bond rotations than 25 with the transition barriers in a range of 10–12 eV.

     PACS numbers: 61.46.+w, 34.10.+x, 81.07.–b

Carbon nanostructures spanning from fullerenes [1] to single and multiwall nanotubes [2], nanopeapods [3], and "Y" and "T" junctions [4] have attracted much attention from scientists for the last two decades due to their unique structural, mechanical, and electrical properties [5]. In particular, carbon nanotubes and related junctions have great potential for applications on nanometric electronic devices such as quantum functional transistors and rectifiers since nanotubes can be semiconductors or metals depending upon their chiralities and diameters [6]. At the moment, however, development of the nanotube-based technology is limited because delicate control of their structures is not yet feasible.

Recently, merging processes between carbon nanostructures have been proposed as a new synthesis technique to construct more complicated functional structures: (i) Two nanotubes coalesce into a diameter-doubled one in a high-energy (1.25 MeV) electron-beam condition [7]. (ii) In the same condition, initially crossed nanotubes are found to form some functional junctions shaped like Y and T characters [4]. Since each carbon atom is displaced approximately every 100 sec by knock-on collisions with the high-energetic electrons, the irradiation-induced vacancies may play a crucial role in these merging processes. Terrones and co-workers [4,7] studied the vacancy-related merging mechanism utilizing the ordinary molecular dynamics technique. Though introducing various functional structures, this high-energy process may not be appropriate for nanometric device application because of uncontrollable defect formation. (iii) A low-energy growth technique for nanotube bundles, where the chiral indexes of all individual nanotubes are almost perfectly monodispersed, was proposed in the mixture of C_{60} molecules and catalyst Ni pillars with a help of a ~1.5 T magnetic field [8]. The annealing temperature is just 950 °C. (iv) In another low-energy situation, a single-wall nanotube can be synthesized by merging fullerene molecules inside a nanotube vessel in nanopeapod systems [9,10]. Of special importance is the last technique of fullerene coalescence because it is a catalyst-free and bottom-up process, having a potential for diameter and chirality control of single-wall nanotubes.

Nanopeapods [3] consist of an array of fullerene molecules (inner peas) and a single-wall carbon nanotube (an outer pod), and all components are separated from the others by the van der Waals distance. The fullerene molecules as one-dimensional crystals are spaced by about 0.97 nm or less, and the filling fraction is over 90%. The high fraction is associated with the exothermic encapsulating process [11,12]. Depending upon preparation methods, the various fullerene species can be C_{60}, C_{70}, C_{82}, and metallofullerenes [3,9,10,13].

Electron-beam irradiation [9] or heat treatment [10] on these carbon composites induces coalescence of core fullerenes into an inside single-wall nanotube, with the diameter being 0.71 nm smaller than that of the outer "vessel" tube. Since the electron-beam in this case is irradiated for hundreds of seconds and its energy is about 0.1 MeV, we cannot expect the irradiation-induced vacancies as in Refs. [4,7]. Actually, the outer wall was little damaged during the coalescence process by the electron beams [9]. Iijima and co-workers baked nanopeapods up to 1200 °C for 14 h. They found that the inside fullerenes start to coalesce at 800 °C and complete transformation to a single-wall nanotube at 1200 °C. They also proposed that diameters of the synthesized nanotubes vary from 0.6 to 0.9 nm depending on the size of the outer vessel tubes in a range of 1.3–1.6 nm [10]. This low-energy merging process of fullerenes has great implication on diameter and chirality control in nanotube growths as we mentioned above, but little is known about its dynamical process. Furthermore, the ordinary molecular dynamics study for the process is not applicable because it never happens within the simulation time when used by the modern supercomputers.

Instead, topological consideration was made by Ueno *et al.* to the case of a C_{120} capsule with (5,5) chiral index

from two dimerized C_{60} fullerenes [14]. They found 22 successive Stone-Wales-type bond rotations as a topologically acceptable pathway for the transformation. Recently, hypothetic transition states between two consecutive local minima of the pathway was examined [15]. Similar topological analysis for head-to-head coalescence of capped nanotubes and fullerenes was made [16]: $(5,5) + (5,5)$, $(10,10) + (10,10)$, and $C_{60} + (10,10)$. However, these do not guarantee real dynamics of the coalescing process beyond topology. Fullerene collision [17,18] and nanotube collision [19] were dealt with molecular dynamics techniques with the assumption of one constituent's high-energetic incidence on the other. Fullerenes packed well inside single-wall nanotubes (nanopeapods) are not relevant with such a high-energetic incidence.

In this Letter, to simulate the low-energy merging process of fullerene molecules with appropriate molecular dynamics information, we use the action-derived molecular dynamics method, recently proposed by Passerone and Parrinello [20] with some modifications for many atom systems [21].

The discretized version [22] of the classical action (S) for numerical simulations is given by

$$S = \sum_{j=0}^{P-1} \Delta(K_j - V_j), \tag{1}$$

where P is the total number of steps for discretization of simulation time τ, $\Delta = \tau/P$ is the constant time interval, and K_j (V_j) are the kinetic (potential) energy of the configuration $\mathbf{q}_j$ at the jth time step. The instantaneous velocity is approximated as $\mathbf{v}_j = (\mathbf{q}_j - \mathbf{q}_{j+1})/\Delta$, and then $K_j = m\mathbf{v}_j^2/2$ where m is the mass of each particle. Dynamical paths can be obtained by finding the stationary point of the action, i.e., $\delta S = 0$, but in general it is a very difficult task to find the stationary point because it involves a root-finding problem which requires the second derivative of the potential. Furthermore, the action is not bounded and the stationary point can be either a local minimum/maximum, or a saddle.

To obtain effectively a dynamical path that is globally close to the Verlet trajectory, i.e., an optimal solution for the discretized action, we employ a rather simple minimization technique, where the action is supplemented with some penalty functions [20,21]:

$$\tilde{\Theta}(\mathbf{q}_j, E; K) = S + \mu_E \sum_{j=0}^{P-1}(E_j - E)^2 + \mu_{\mathbf{P}} \sum_{j=0}^{P-1} \mathbf{P}_j^2$$
$$+ \mu_{\mathbf{L}} \sum_{j=0}^{P-1} \mathbf{L}_j^2 + \mu_K(\langle K_j \rangle - K)^2. \tag{2}$$

Here, $\mathbf{P}_j$ ($\mathbf{L}_j$) is the instantaneous total linear (angular) momentum, and $E_j = K_j + V_j$ is the instantaneous total energy of N particles at step index j. E and K is the target total and kinetic energy, respectively, and all the μ's are numerical parameters that enforce the corresponding constraints. The $\langle \cdots \rangle$ means the time average. With μ_E,

$\mu_{\mathbf{P}}$, and $\mu_{\mathbf{L}}$, we enforce the conservation laws of total energy, and total linear/angular momenta on the optimized trajectory. The last term in Eq. (2) is associated with the virial theorem that classical trajectories should satisfy, causing thermal motions around potential basins; in thermodynamic language, the virial theorem corresponds to the equipartition theorem.

In our action-derived molecular dynamics simulations, we minimize the generalized action $\tilde{\Theta}$ with respect to various atomic paths using a conjugate gradient technique for the given initial and final N-atom configurations, as shown in Fig. 1. The potential energy and Hellmann-Feynman forces are calculated using a tight-binding model for carbon systems [23]. Details of formulation and numerical procedure will be presented elsewhere [21].

For the fullerene coalescing process, we can reasonably assume that its initial state is two C_{60} molecules separated by ~1 nm [9,10]. However, for the final configuration, we can expect various C_{120} nanocapsules with different diameters and chiralities because experimentally the diameters of the synthesized inner tubes range in 0.6–0.9 nm [10]. The simplest case is the C_{120} nanocapsule with a diameter of 0.7 nm and chiral index of (5,5) [hereafter we call it the (5,5) nanocapsule], as other workers considered [14–16]. We also present a possible diameter thickening process by forming (10,0), (6,6), and (12,0) nanocapsules with diameters of 0.8–9.8 nm, as shown in Fig. 1. Assuming that all the atoms move least distance from initial to final states in order to accelerate the numerical convergence, we choose the
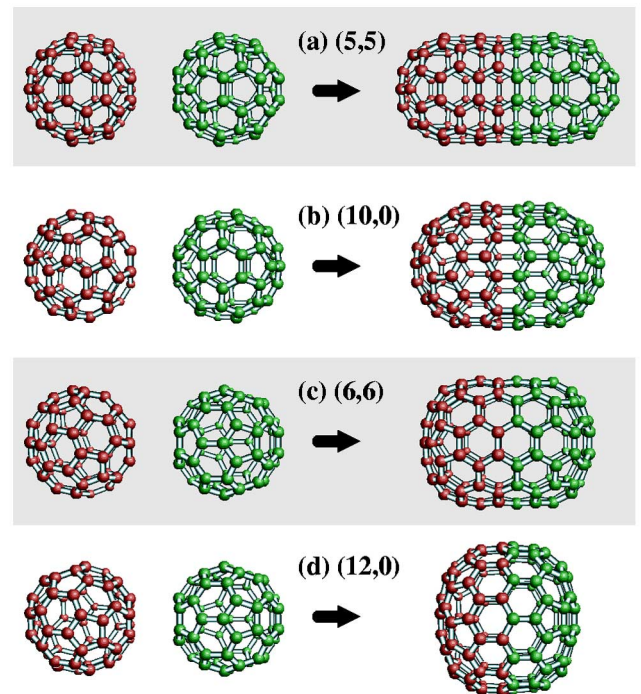

FIG. 1 (color online). Initial and final states for forming various C_{120} nanocapsules as precursors for fullerene-based nanotube growth.

initial orientation of two fullerene molecules differently depending on the cap structure of the final nanocapsules. With this we can remove free rotational motion of a single molecule in the full molecular dynamics simulation, while saving much computation time.

We perform action-derived molecular dynamics simulations using the parameters of $\mu_E = 10^8$, $\mu_P = \mu_L = \mu_K = 10^4$, $P = 199$, and $\tau = P\Delta = 1.2$ ps, and display the results in Fig. 2. With the numerical parameters, we find that the total energy is well conserved over all time steps for all the nanocapsules, whereas the linear and angular momenta is well converged for the (5,5) and (10,0) capsules, but less strictly for (6,6) and (12,0) capsules. Since E and K cannot be an independent variable in a microcanonical problem where total energy of systems is conserved, we relax K within the minimization technique, regarding it as an extra variable after achieving some convergence.
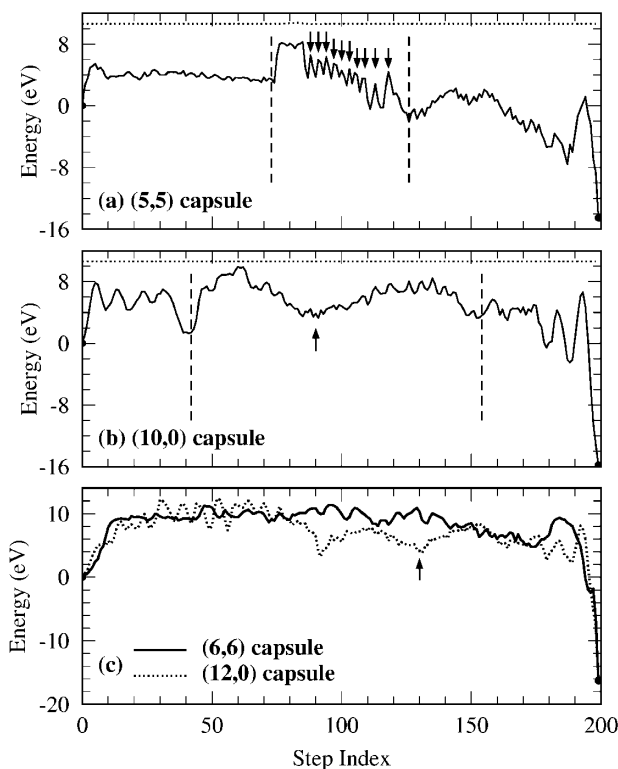

FIG. 2. Potential energy variation along the obtained dynamical trajectories of fullerene coalescence for forming various C_{120} nanocapsules. In (a) and (b), the solid (dotted) lines indicate the potential (total) energy of the (5,5) and (10,0) capsules, respectively, along the time step. We divide the trajectories into three parts as reactant, activation, and product regions in series. In (a), ten small arrows correspond to ten Stone-Wales-type bond rotations. In (b), the single arrow indicates when the intermediate (5,5) capsule arises. In (c), we depict the potential energy variation in the case of the (6,6) and (12,0) C_{120} capsules. Also, the small arrow indicates the forming of the intermediate (6,6) capsule in the trajectory of the (12,0) capsule.

For the coalescing process of the two C_{60} molecules into the (5,5) C_{120} nanocapsule, we can divide the obtained dynamical trajectory into three parts as reactant, activation, and product regions in series [24], as in Fig. 2(a). In the reactant region around the initial configuration, the 120 atoms of the two C_{60} molecules are randomly vibrated around their energy minima with preserving fullerene cage structures. This motion can be regarded as thermal motion, and be consistent with random trajectories around potential minima of the Mueller potential in Ref. [20]. The relation $\langle K_j \rangle \approx \langle \triangle V_j \rangle$, the virial theorem for the harmonic potential, is satisfied. In the product region near the final state, we similarly find a thermal vibrating motion of the (5,5) C_{120} nanocapsule. The coalescence occurs in between, i.e., the activation region of about 0.3 ps. At the transition state, two fullerenes start to merge with breaking some C-C bonds to open cage, and then a peanut-shaped intermediate structure appears at step index 87. Then, we can see ten successive Stone-Wales-type bond rotations forming small potential peaks due to the occurrence of under-coordinated carbon atoms. The ten rotations are attributed to the fivefold symmetry of the initial and final states, as discussed in Ref. [16]. The peak height is about 2–5 eV. For the whole coalescence process, the energy barrier is estimated to 8.3 eV. This is quite comparable to the energy barrier for single Stone-Wales transformation in a C_{60} molecule [25].

For the (10,0) nanocapsule, we also find the reactant and product regions of the dynamical trajectory with randomly vibrating atomic motion around both the potential basins. We count about 25 Stone-Wales-type bond rotations in between activation regions, lasting about 0.6 ps to complete the transformation. An intermediate (5,5) C_{120} nanocapsule is found at step index 90 on the trajectory for the (10,0) capsule, indicated by the arrow in Fig. 2(b). Thus, we find a transformation route: two C_{60} fullerenes $\rightarrow$ (5,5) C_{120} nanocapsule $\rightarrow$ (10,0) C_{120} nanocapsule. In the former part, a transition state occurs with an energy barrier of 9.9 eV, taking about ten bond rotations, and in the latter part the (5,5) nanocapsule transforms into (10,0) nanocapsule through about 15 bond rotations, with an energy barrier of less than 8 eV. Even though the former process is conceptually similar to the coalescence process for forming (5,5) nanocapsule of Fig. 2(a), the energy barrier is higher by 1.6 eV because of the difference in the initial molecular orientation, as shown in Figs. 1(a) and 1(b).

In the cases of (6,6) and (12,0) nanocapsules, the whole processes require more bond rotations than 30. With the simulation time of 1.2 ps, the obtained dynamical trajectories shown in Fig. 2(c) entirely belong to the activation process, different from those for the (5,5) and (10,0) nanocapsules in Figs. 2(a) and 2(b). If we use sufficiently large τ to cover 30–60 bond rotations, we may get such thermal vibrating modes near the initial and final states, but this demands much computational cost. With the

TABLE I. Fullerene coalescence into various C_{120} nanocapsules. Diameter of capsules (D), formation energy (H_f), overall potential energy barriers (V_b), average kinetic energy in Kelvin ($\langle K_j \rangle$), and O values are compared for the used target energy (E).

	D (Å)	H_f (eV)	V_b (eV)	$\langle K_j \rangle$ (K)	O (a.u.)	E (a.u.)
(5,5)	6.85	−14.53	8.3	556	599.5	−29.85
(10,0)	8.02	−15.81	9.9	360	368.9	−29.85
(6,6)	8.32	−16.25	11.4	239	227.7	−29.80
(12,0)	9.78	−16.30	12.4	353	300.7	−29.78

limited simulation time, even though we can not guarantee the real dynamics (in fact, total linear/angular momenta are poorly conserved), we can estimate satisfactorily activation energy barriers within the action-derived molecular dynamics formalism. The calculated values are 11.4 (step index 97) and 12.4 eV (step index 50) for the (6,6) and (12,0) nanocapsules, respectively, rather high compared to those for the (5,5) and (10,0) nanocapsules. The limited simulation time causes the simultaneous Stone-Wales-type bond rotations, resulting in the high-energy barriers. Another reason is that, since we preserve the sixfold symmetry in the initial and final states of these systems, double bonds of the hexagons should be broken to coalesce initially. This initial opening process needs an energy cost of about 10 eV, which corresponds to step index 0–30. We also find an intermediate (6,6) nanocapsule at step index 130 in the path of forming the (12,0) nanocapsule, indicated by the arrow in Fig. 2(c).

We summarize all results and the target energy (E) used for these four nanocapsules in Table I. As the diameters increase, the capsules are more stable with relaxing strain energy, but estimated energy barriers are higher. The large energy barriers over 10 eV in the cases of the (6,6) and (12,0) nanocapsules are attributed to the limited simulation time and thus simultaneous bond rotations. Our estimated values for transition barriers are quite reasonable for a low-energy merging process of fullerenes inside single-wall nanotubes. The value of 10 eV corresponds to a system temperature of 1450 K for two C_{60} molecules, and the experimental temperature for the merging process is 1500 K [10]. We also display the average kinetic energy $\langle K_j \rangle$ used for ensuring the virial theorem, and the discretized Onsager-Machlup actions O [26]. The obtained O values are rather large, especially for the cases of the (5,5) nanocapsule due to the thermal motions in dynamical trajectory. We note that the action-derived molecular dynamics cannot offer a unique solution for the dynamical paths of a specific rare event. We may obtain different dynamical paths with various O and $\langle K_j \rangle$, depending on the target energy, initial seed, and minimization schedule for the functional Eq. (2). Nevertheless, we believe that the $\bar{\Theta}$ trajectory generally reflects the real dynamics of the system under consideration via

the constraints for the classical laws. By imposing the appropriate dynamical laws and virial theorem, we can obtain an estimate, and not exact value, for transition energy barrier and transformation processes for specific rare events based on the real dynamics.

In conclusion, we investigate the molecular transformation of two C_{60} fullerenes into various C_{120} nanocapsules, and find dynamical paths for the fullerene coalescence using the action-derived molecular dynamics technique. In the dynamical process of forming the various C_{120} nanocapsule with the chiral indexes of (5,5), (10,0), (6,6), and (12,0), we find that the process consists of successive Stone-Wales-type bond rotations with the transition energy barrier of about 8–12 eV. Further growth via coalescence between nanocapsules and C_{60} fullerenes may be natural extension of the above coalescence process with great similarity, requiring future study.

---

*Electronic address: yonghyun@mail.kaist.ac.kr
[1] H.W. Kroto *et al.*, Nature (London) **318**, 162 (1985).
[2] S. Iijima, Nature (London) **354**, 56 (1991).
[3] B.W. Smith *et al.*, Nature (London) **396**, 323 (1998).
[4] M. Terrones *et al.*, Phys. Rev. Lett. **89**, 075505 (2002).
[5] M.S. Dresselhaus *et al.*, *Science of Fullerenes and Carbon Nanotubes* (Academic, San Diego, 1996).
[6] C. Dekker, Phys. Today **52**, No. 5, 22 (1999).
[7] M. Terrones *et al.*, Science **288**, 1226 (2000).
[8] R.R. Schlittler *et al.*, Science **292**, 1136 (2001).
[9] D.E. Luzzi and B.W. Smith, Carbon **38**, 1751 (2000).
[10] S. Bandow, *et al.*, Chem. Phys. Lett. **337**, 48 (2001).
[11] S. Okada *et al.*, Phys. Rev. Lett. **86**, 3835 (2001).
[12] S. Berber *et al.*, Phys. Rev. Lett. **88**, 185502 (2002).
[13] K. Hirahara *et al.*, Phys. Rev. Lett. **85**, 5384 (2000).
[14] H. Ueno *et al.*, Fullerene Sci. Technol. **6**, 319 (1998).
[15] M. Yoon *et al.* (to be published).
[16] Y. Zhao *et al.*, Phys. Rev. Lett. **88**, 185501 (2002).
[17] B.L. Zhang *et al.*, J. Phys. Chem. B **97**, 3134 (1993).
[18] Y. Xia *et al.*, Phys. Rev. B **53**, 13 871 (1996).
[19] T. Kawai *et al.*, Phys. Rev. Lett. **89**, 085901 (2002).
[20] D. Passerone and M. Parrinello, Phys. Rev. Lett. **87**, 108302 (2001).
[21] Y.-H. Kim *et al.* (to be published).
[22] R.E. Gillilan and K.R. Wilson, J. Chem. Phys. **97**, 1757 (1992).
[23] C.H. Xu *et al.*, J. Phys. Condens. Matter **4**, 6047 (1992).
[24] See EPAPS Document No. E-PRLTAO-90-021305 for video of trajectories divided into three parts as reactant, activation, and product regions in series. A direct link to this document may be found in the online article's HTML reference section. The document may also be reached via the EPAPS homepage (http://www.aip.org/pubservs/epaps.html) or from ftp.aip.org in the directory /epaps/. See the EPAPS homepage for more information.
[25] J.-Y. Yi and J. Bernholc, J. Chem. Phys. **96**, 8634 (1992).
[26] R. Olender and R. Elber, J. Chem. Phys. **105**, 9299 (1996).